Electronic Supplementary Information (ESI)

A multifunctional Zr(IV)-based metal-organic framework for highly efficient elimination of Cr(VI) in aqueous phase

Junmin Liu[#], Yu Ye[#], Xiaodong Sun, Bing Liu, Guanghua Li, Zhiqiang Liang* and Yunling Liu*

State Key Laboratory of Inorganic Synthesis and Preparative Chemistry, College of Chemistry, Jilin University, Changchun 130012, P. R. China
E-mail: yunling@jlu.edu.cn; liangzq@jlu.edu.cn

S1. Calculation procedures of selectivity from IAST

The measured experimental data is excess loadings (q^{ex}) of the pure components CO_2, C_2H_2, C_2H_4, CH_4, C_2H_6 and C_3H_8 for **JLU- MOF60**, which should be converted to absolute loadings (q) firstly.

$$q = q^{ex} + \frac{pV_{pore}}{ZRT}$$

Here Z is the compressibility factor. The Peng-Robinson equation was used to estimate the value of compressibility factor to obtain the absolute loading, while the measure pore volume 0.56 cm^3 g^{-1} is also necessary.

The dual-site Langmuir-Freundlich equation is used for fitting the isotherm data at 298 K.

$$q = q_{m_1} \times \frac{b_1 \times p^{1/n_1}}{1 + b_1 \times p^{1/n_1}} + q_{m_2} \times \frac{b_2 \times p^{1/n_2}}{1 + b_2 \times p^{1/n_2}}$$

Here p is the pressure of the bulk gas at equilibrium with the adsorbed phase (kPa), q is the adsorbed amount per mass of adsorbent (mol kg^{-1}), q_{m1} and q_{m2} are the saturation capacities of sites 1 and 2 (mol kg^{-1}), b_1 and b_2 are the affinity coefficients of sites 1 and 2 (1/kPa), n_1 and n_2 are the deviations from an ideal homogeneous surface.

The selectivity of preferential adsorption of component 1 over component 2 in a mixture containing 1 and 2, perhaps in the presence of other components too, can be formally defined as

$$S = \frac{q_1/q_2}{p_1/p_2}$$

q_1 and q_2 are the absolute component loadings of the adsorbed phase in the mixture. These component loadings are also termed the uptake capacities. We calculate the values of q_1 and q_2 using the Ideal Adsorbed Solution Theory (IAST) of Myers and Prausnitz.

S2. Synthesis of 2,3,5,6-Tetrakis(4-carboxyphenyl)pyrazine

Vitamin B1 (1.1 g, 0.81mmol), CH_3OH (18 mL) and H_2O (6 mL) was added to a 150 mL round-bottomed flask, 2 mol NaOH aqueous solution was added drop by drop to adjust the pH to 9, before methyl 4-formylbenzoate (9.0 g, 54.87 mmol) was added. The mixture was stirred for 1 h in ice water; the reaction was then gradually heated to 85 °C and keep for 4 h. And the crude precipitate was filtered, washed with water and dried at an 80 °C oven. The obtained product (6.50 g, 20.00 mmol) and ammonium acetate (5 g, 60.00 mmol) was dissolved in acetic acid (20 mL), acetic anhydride (3.01 g, 30.00 mmol) was then introduced. The solution was heated at 120 ^{o}C and refluxed under the nitrogen for 3 days, and the precipitate was collected by filtration and washed with water and diethyl ether several times, respectively. 2,3,5,6-tetrakis(4-(methoxycarbonyl)phenyl)pyrazine as a yellow solid was obtained without further characterization. The obtained ester (4.00 g) and power NaOH (3.20 g, 79.60 mmol) was placed in the mixture of 60 mL THF and 60 mL H_2O. The solution was then refluxed overnight. After cooling to room temperature, THF was evaporated. The remaining aqueous solution was acidized to pH = 4 with dilute HCl. The resulting precipitate was filtered, washed with water and dried to afford H_4TCPP as yellow solid. As shown in Fig. S1, ^{1}H NMR (300MHz, DMSO-$_{d6}$): δ = 13.11 (br, 4 H), 7.97 (d, J = 8.6 Hz, 8 H), 7.69 (d, J = 8.6 Hz, 8 H).

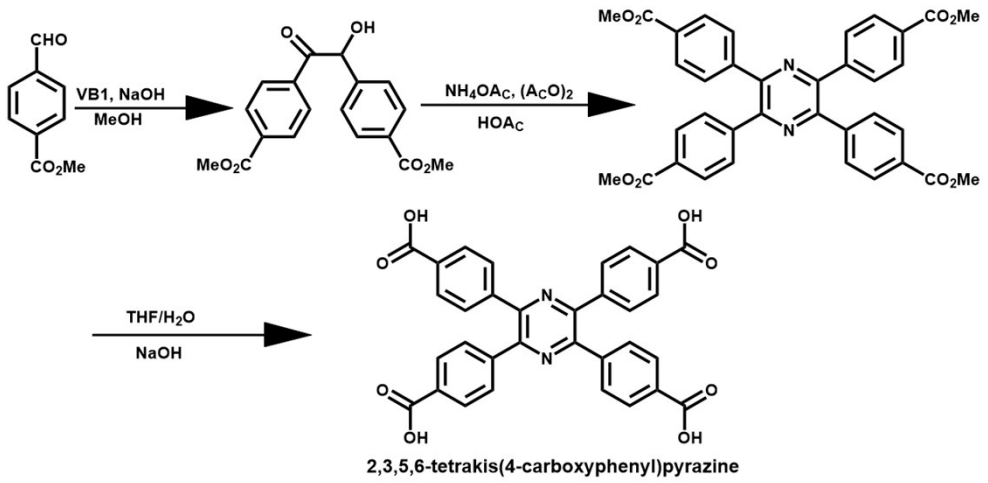

Scheme S1 The synthesis of ligand 2,3,5,6-tetrakis(4-carboxyphenyl)pyrazine (H_4TCPP).

S3. Supporting Figures

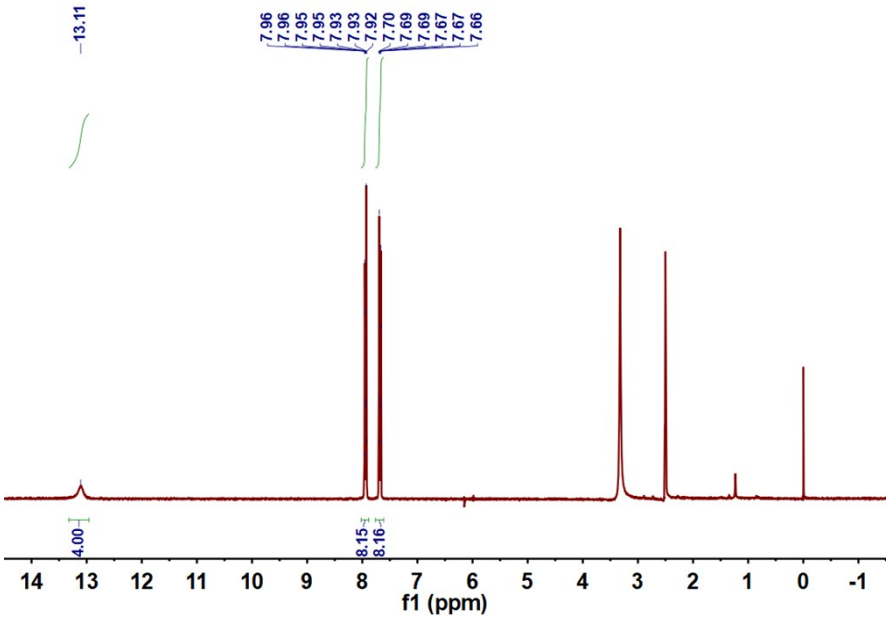

Fig. S1 ^{1}H NMR spectrum of 2, 3, 5, 6-tetrakis (4-carboxyphenyl)pyrazine.

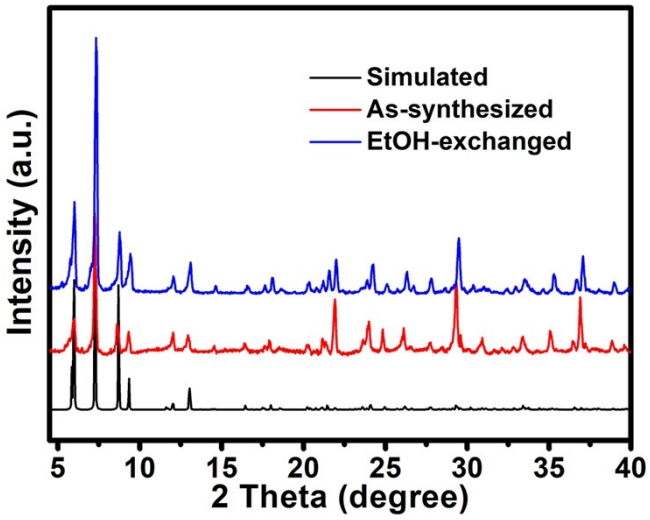

Fig. S2 PXRD patterns of **JLU-MOF60** for the simulated, as-synthesized and EtOH exchanged samples.

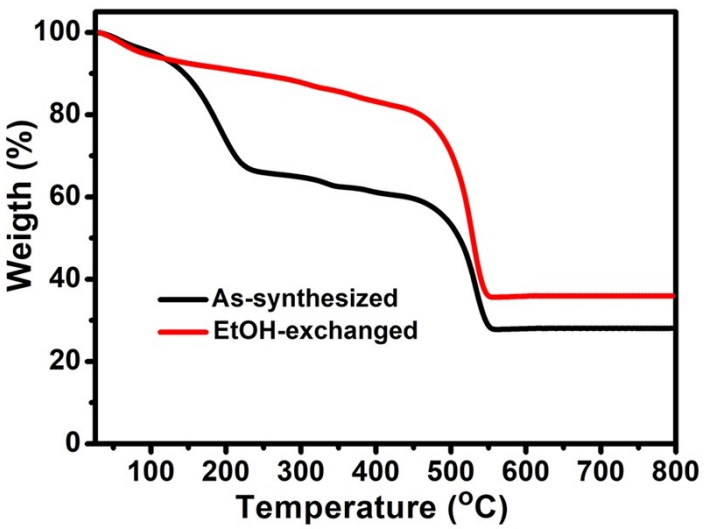

Fig. S3 TGA curves of **JLU-MOF60** for the as-synthesized and EtOH exchanged samples.

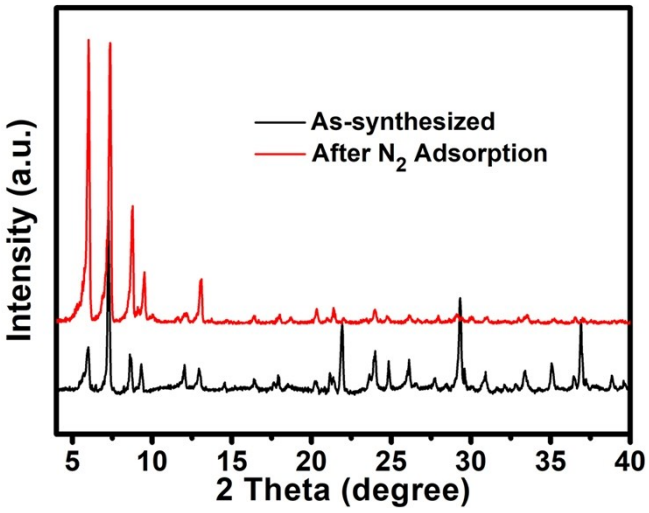

Fig. S4 PXRD patterns of **JLU-MOF60** for the simulated samples and the samples after N_2 adsorption.

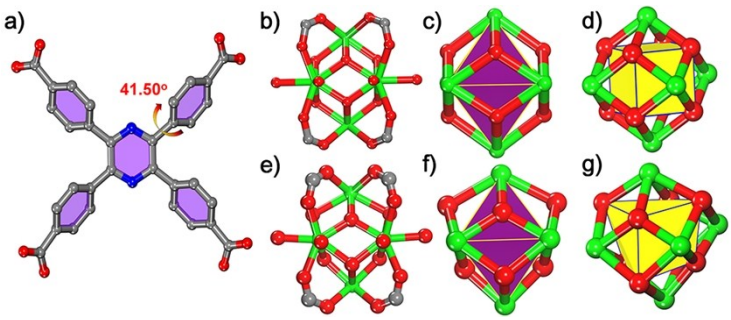

Fig. S5 (a) The dihedral angle between benzene rings and pyrazine ring in H_4TCPP, (b) and (e) $Zr_6O_4(OH)_8(H_2O)_4(COO)_8$ SBU in **BUT-12** and **JLU-MOF60**, respectively, (c) The idealized $Zr_6O_4(OH)_4$ cluster core and Zr_6 octahedron (purple) in **BUT-12**, (d) The regular $(\mu_3\text{-O})_8$ cube (yellow) of **BUT-12**, (f) the irregular $Zr_6O_4(OH)_4$ cluster core and Zr_6 octahedron (purple) in **JLU-MOF60**, (g) The irregular $(\mu_3\text{-O})_8$ polyhedron (yellow) (grey, C, red, O, red, blue, N, green, Zr, H atoms on ligands are omitted).

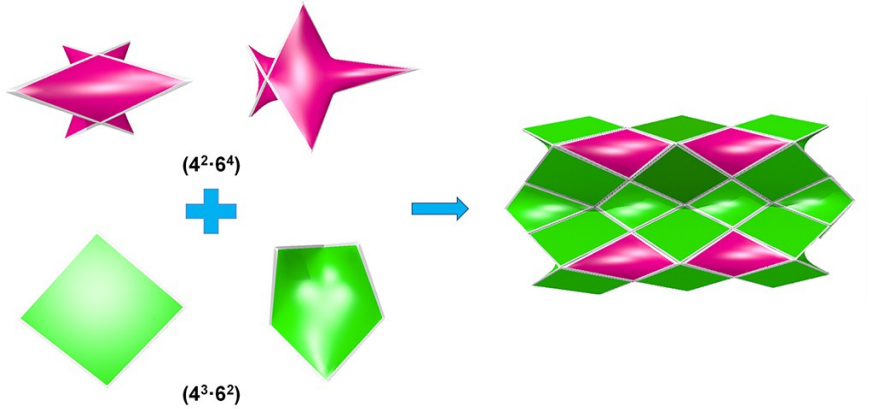

Fig. S6 Topological feature of **JLU-MOF60** displayed by tiles, and two kinds of point symbols for gold and purple tiles are $(4^2 \cdot 6^4)$ and $(4^3 \cdot 6^2)$, respectively.

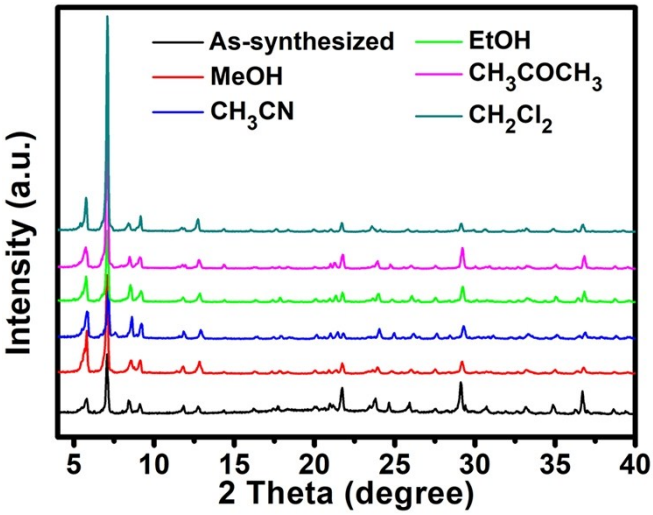

Fig. S7 PXRD patterns of **JLU-MOF60** samples immersed in different organic solutions for 48 h.

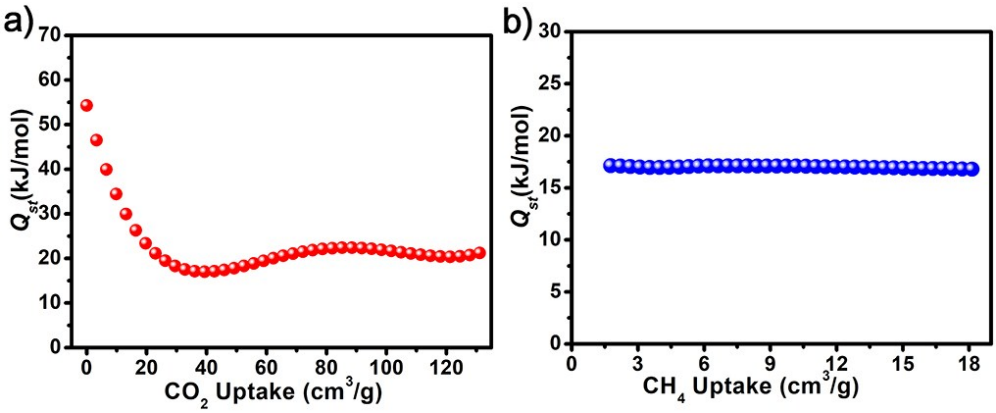

Fig. S8 (a) Q_{st} of CO_2 at zero loading, (b) Q_{st} of CH_4 for **JLU-MOF60**.

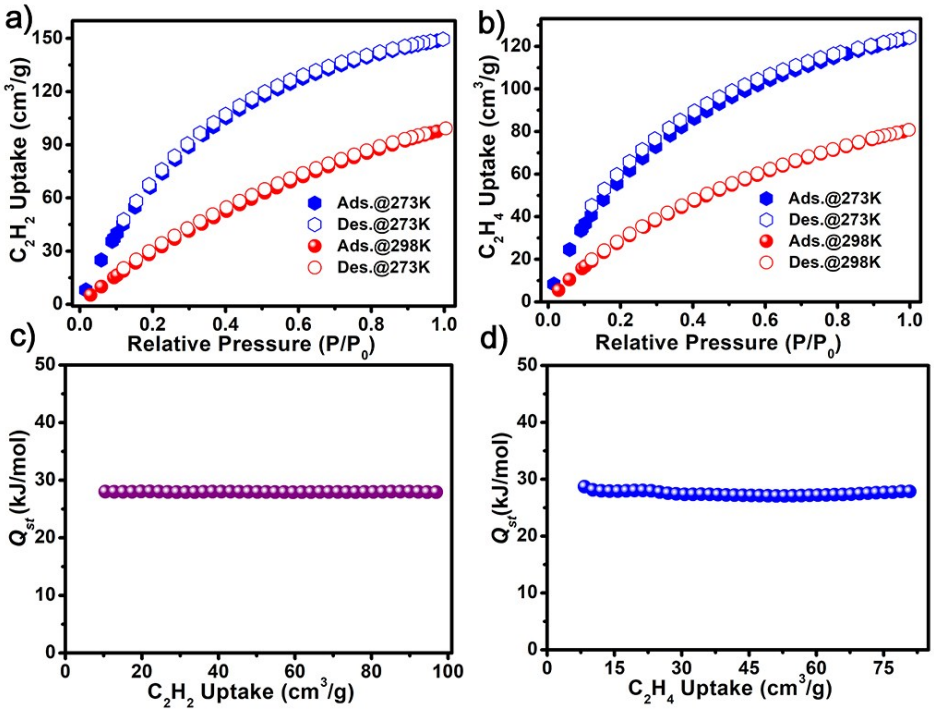

Fig. S9 (a) C_2H_2 and (b) C_2H_4 adsorption isotherms at 273 and 298 K, respectively, (c) Q_{st} of C_2H_2 and (d) C_2H_4 for **JLU-MOF60**.

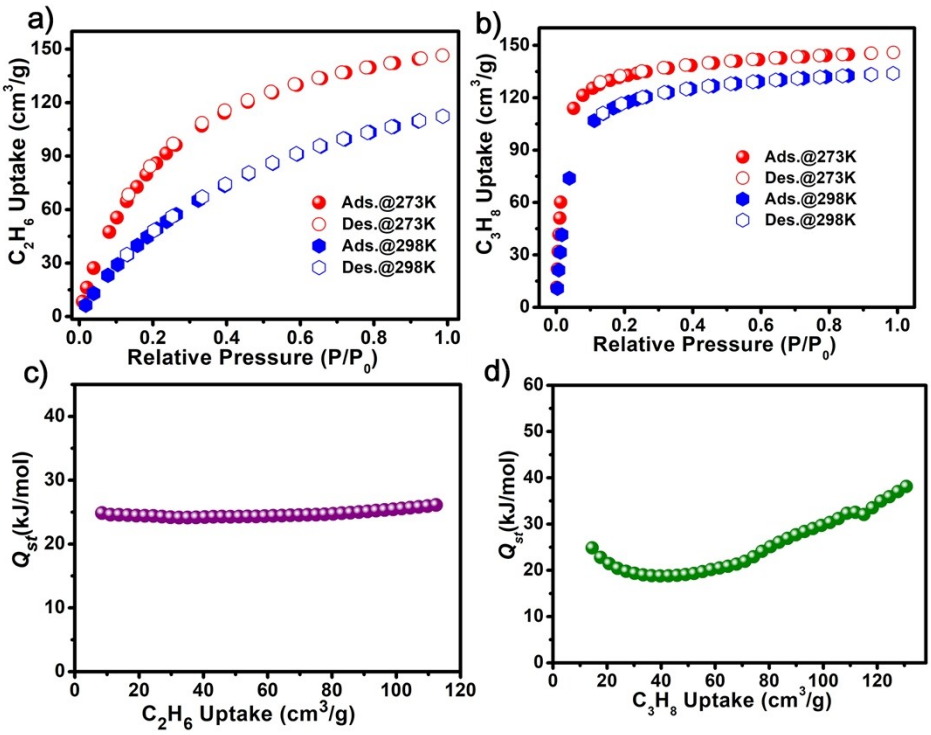

Fig. S10 (a) C_2H_6 and (b) C_3H_8 adsorption isotherms, (c) Q_{st} of C_2H_6 and (d) C_3H_8 for **JLU-MOF60** at 273 and 298 K under 1 bar.

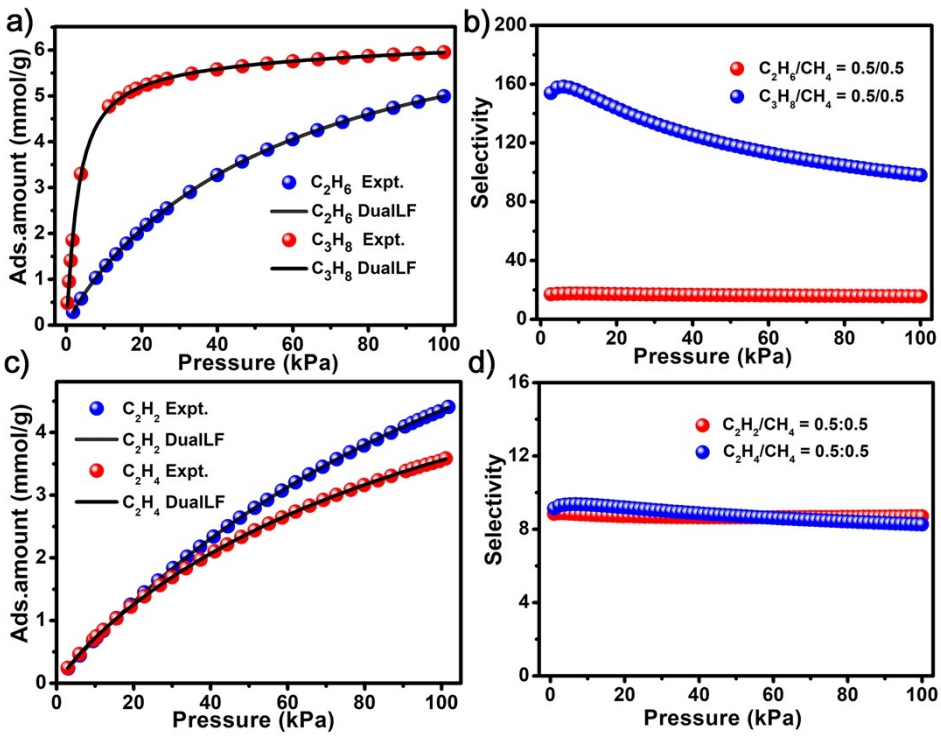

Fig. S11 (a) C_2H_6 and C_3H_8 and (c) C_2H_2 and C_2H_4 adsorption isotherms at 298 K along with the dual-site Langmuir Freundlich (DSLF) fits. The gas mixture adsorption selectivity of (b) C_2H_6/CH_4 and C_3H_8/CH_4 and (d) C_2H_2/CH_4 and C_2H_4/CH_4 are predicted by IAST at 298 K and 100 kPa for **JLU-MOF60**.

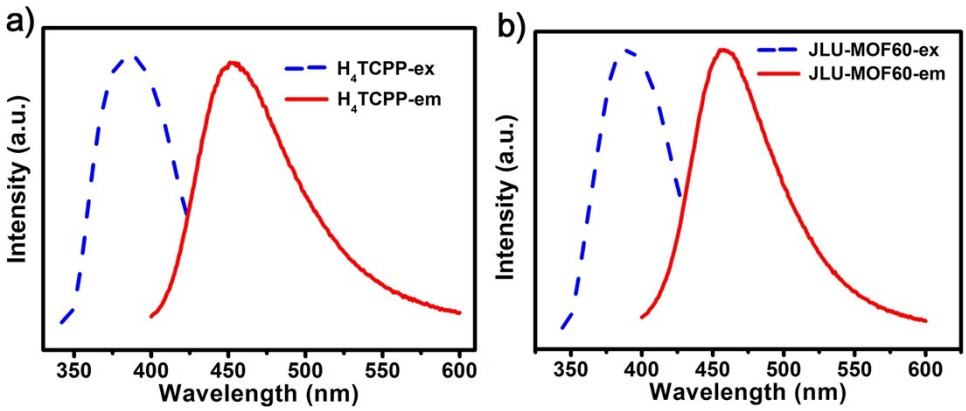

Fig. S12 (a) The solid-state excitation (dot lines) and emission (solid lines) spectra of H_4TCPP ligand with emission peaks at 450 nm under excitation of 385 nm. (b) The solid-state excitation (dot lines) and emission (solid lines) spectra of **JLU-MOF60** with emission peaks at 450 nm under excitation of 385 nm.

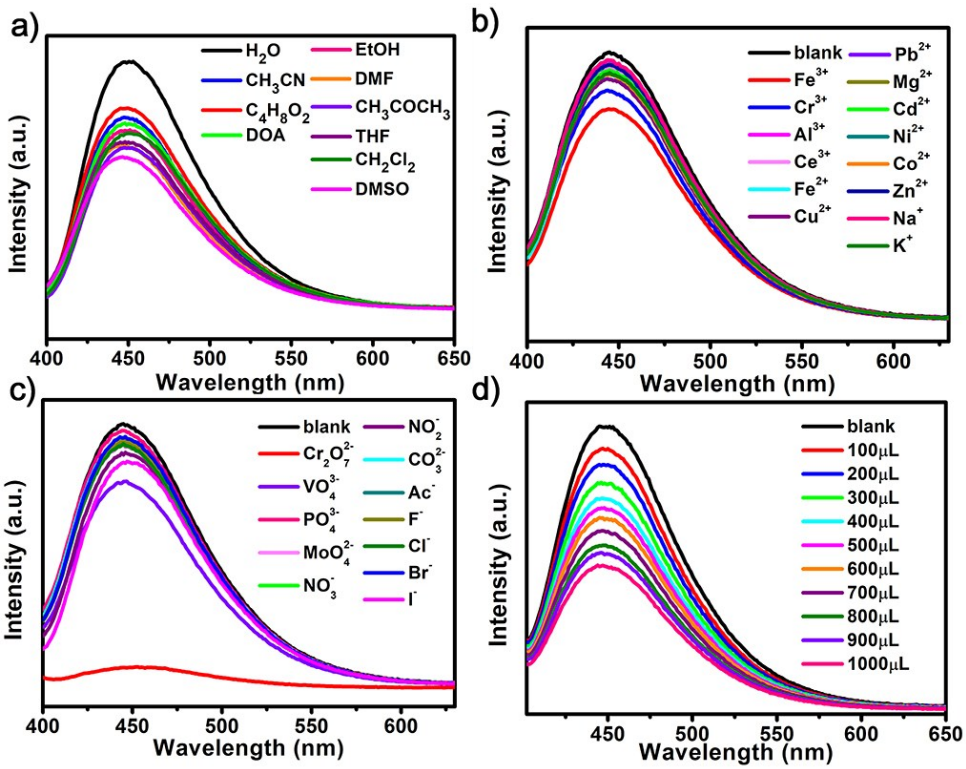

Fig. S13 Luminescent spectra of **JLU-MOF60** suspensions in the presence of different solutions (a), cations (b) and anions (c) under excitation of 385 nm, respectively. (d) Effect on the emission spectra of **JLU-MOF60** dispersed in water with the incremental addition of 1 mmol UO_2^{2+} aqueous solution.

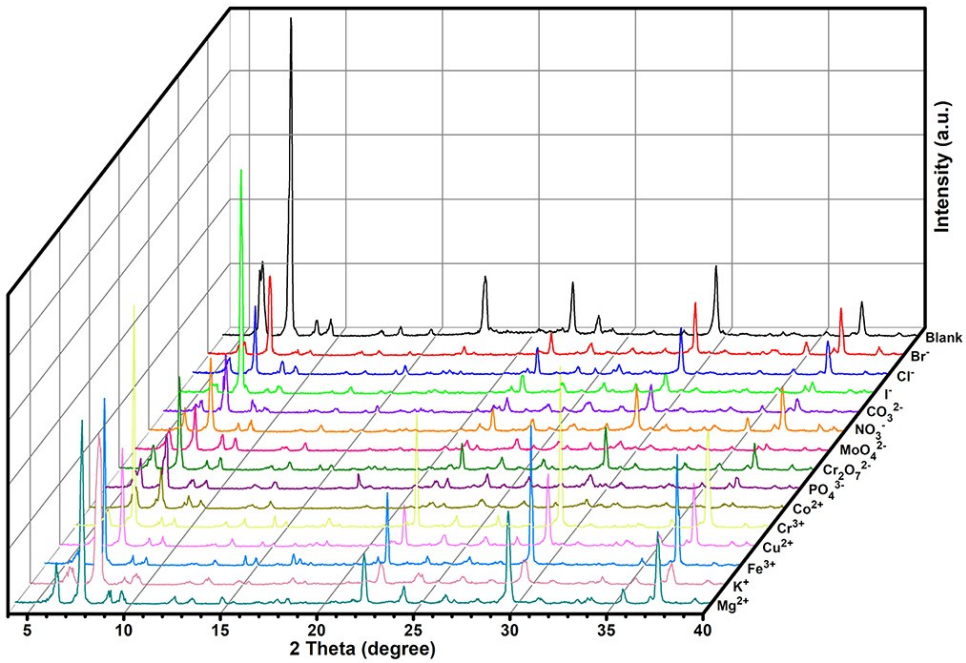

Fig. S14 PXRD patterns of samples soaked in different cations and anions.

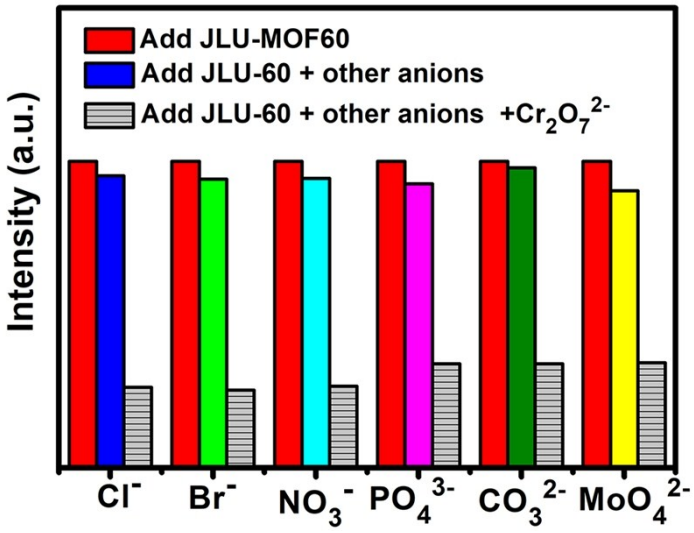

Fig. S15 The selective detection of $Cr_2O_7^{2-}$ on **JLU-MOF60** in the presence of other anions in the water (red bars: Fluorescence intensity of **JLU-MOF60** dispersed in the water; multicolor bars: Fluorescence intensity of **JLU-MOF60** dispersed in the water with the addition of 100 μL 10 mmol different anions; grey bars: Fluorescence intensity of **JLU-MOF60** dispersed in the water with the addition of 100 μL 10 mmol different anions and 100μL 1 mmol $Cr_2O_7^{2-}$ solutions).

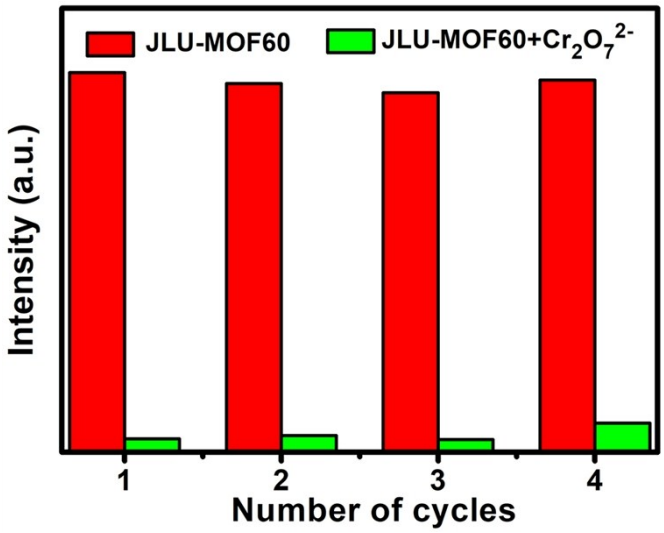

Fig. S16 Four cycles of the quenching effect of **JLU-MOF60** in the presence of 200 μL 1mmol $Cr_2O_7^{2-}$ solutions.

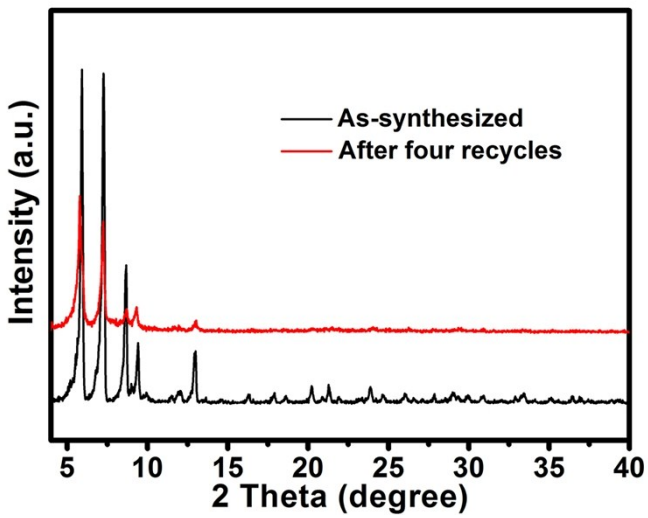

Fig. S17 PXRD patterns of the as-synthesized samples and the samples after four fluorescence detection cycles.

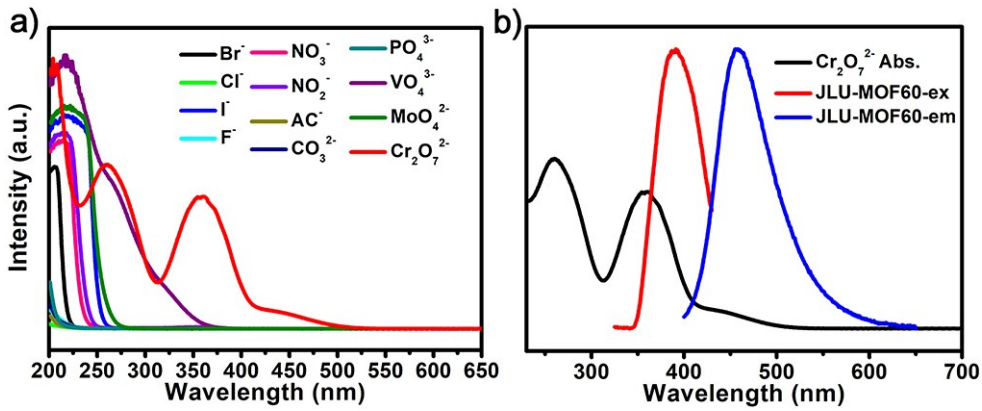

Fig. S18 (a) UV-vis spectra of different anions in aqueous solutions, (b) the overlap between the emission and excitation spectra of the **JLU-MOF60** and the absorption spectrum of $Cr_2O_7^{2-}$ solutions.

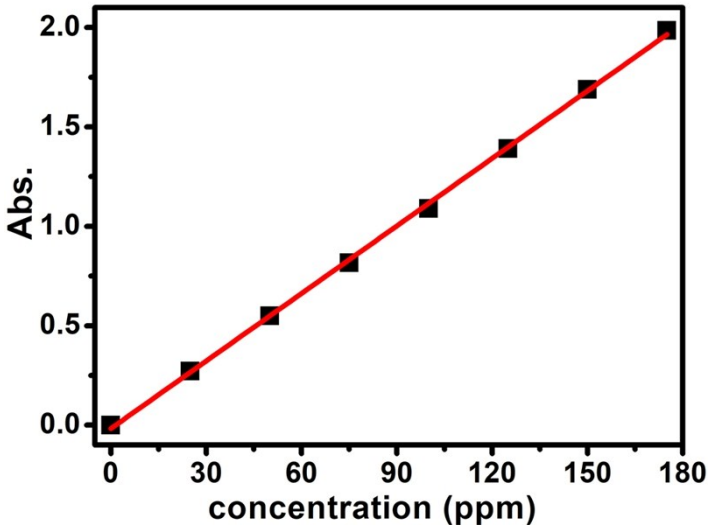

Fig. S19 The standard curve line of $Cr_2O_7^{2-}$ was performed and the concentration of $Cr_2O_7^{2-}$ has a good linear relationship with its absorbance ($R^2 > 0.999$).

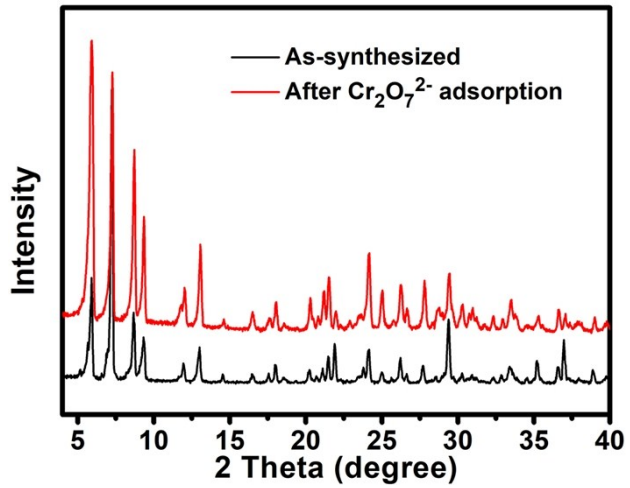

Fig. S20 PXRD patterns for **JLU-MOF60** samples before and after the measurements of $Cr_2O_7^{2-}$ adsorption.

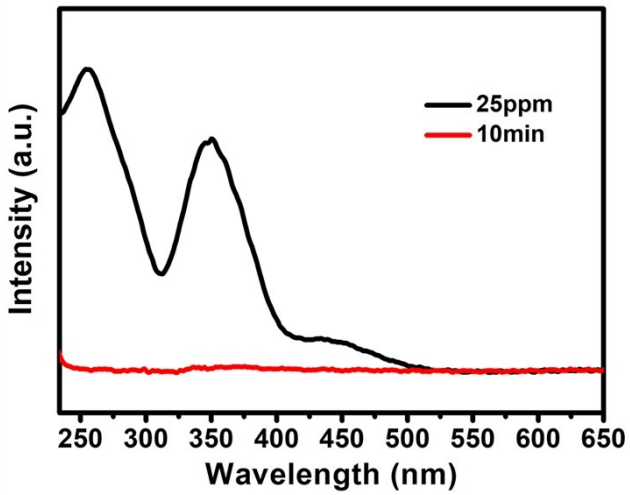

Fig. S21 UV-vis spectra for the $Cr_2O_7^{2-}$ adsorption behavior of **JLU-MOF60** at low concentration (25 ppm).

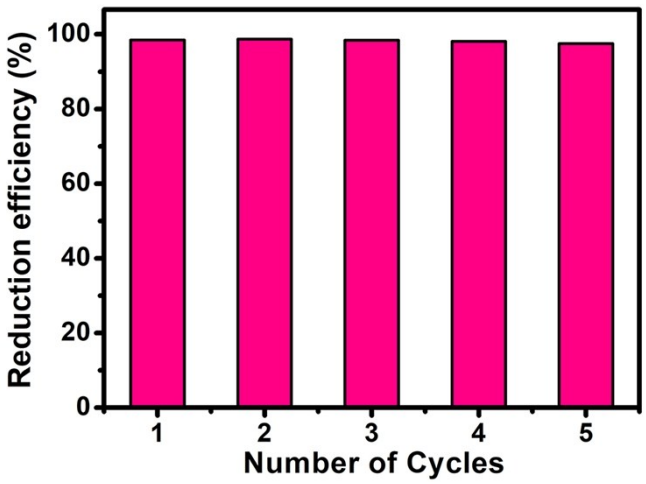

Fig. S22 Cycles test of photocatalytic reduction of Cr(VI) using **JLU-MOF60**.

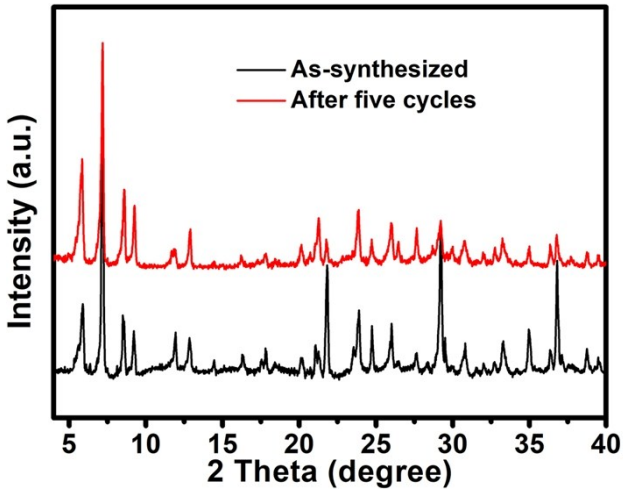

Fig. S23 PXRD patterns of the as-synthesized samples and the samples after five photocatalytic reduction cycles.

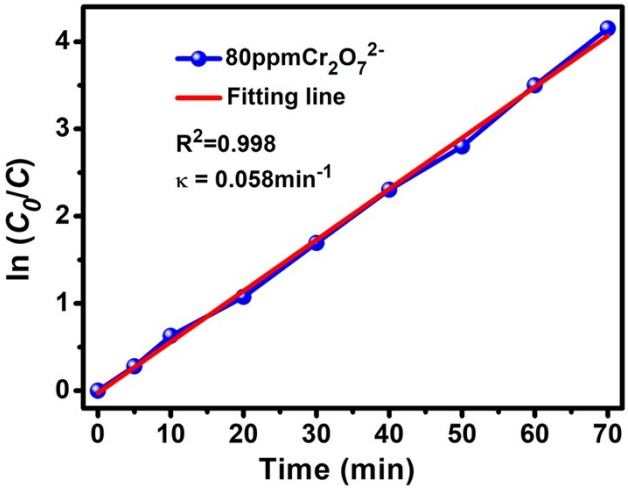

Fig. S24 The apparent rate constant plot for **JLU-MOF60** during the photocatalytic reduction reaction.

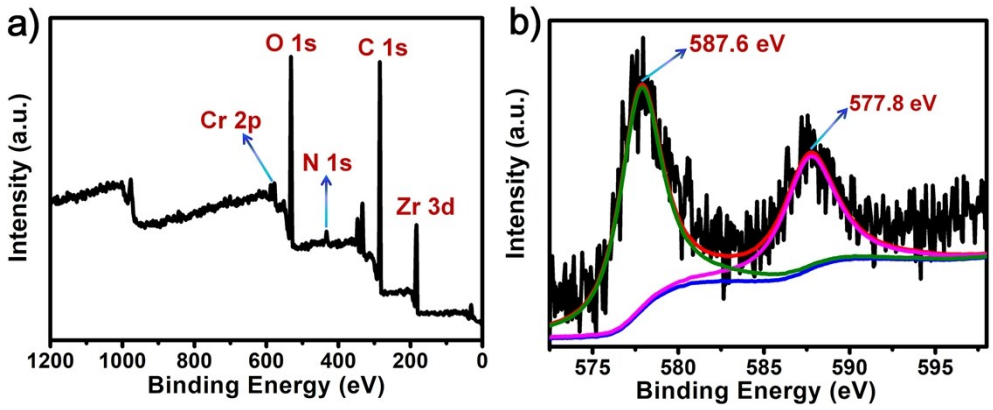

Fig. S25 (a) XPS survey spectrum of **JLU-MOF60** after photocatalytic reduction reaction, (b) high-resolution Cr 2p spectrum: the two peaks at 577.8 and 587.6 eV are assigned to the $2p_{3/2}$ and $2p_{1/2}$ of Cr(III), which reveals the reduction of Cr(VI) to Cr(III).

S3. Supporting Tables

Table S1. Crystal data and structure refinement for **JLU-MOF60**

formula	C_{91} H_{118} N_{13} $O_{44.50}$ Zr_6
formula weight	2653.30
temp (K)	293(2) K
wavelength (Å)	0.71073 Å
crystal system, space group	Tetragonal, $I4_1/amd$
a (Å)	15.246(2)
b (Å)	15.246(2)
c (Å)	60.403(12)
V (Å^3)	14039(4)
Z, D_c (Mg/m^3)	4, 1.255
F(000)	5404
θ range (deg)	2.99 to 25.11°
reflns collected/unique	54313/3386
R_{int}	0.0634
data/restraints/params	3386/1/129
GOF on F^2	1.145
R_1, wR_2 (I>2σ(I))	R_1 = 0.0395, wR_2 = 0.1117
R_1, wR_2 (all data)	R_1 = 0.0536, wR_2 = 0.1185

Table S2. Selected bond lengths [Å] and angles [º] for **JLU-MOF60**.

Zr(1)-O(2)	2.0707(15)	O(1)-Zr(1)#1	2.2401(18)
Zr(1)-O(2)#1	2.0707(15)	O(1)-H(1)	0.987(19)
Zr(1)-O(5)	2.196(3)	O(2)-Zr(1)#3	2.0707(15)
Zr(1)-O(5)#2	2.196(3)	O(3)-C(8)	1.263(4)
Zr(1)-O(1)	2.2401(18)	O(4)-C(8)	1.261(4)
Zr(1)-O(1)#3	2.2401(18)	N(1)-C(1)#7	1.338(4)
Zr(1)-O(3)#2	2.243(2	N(1)-C(1)	1.338(4)
Zr(1)-Zr(2)	3.5136(7)	C(1)-C(1)#8	1.395(7)
Zr(1)-Zr(2)#1	3.5136(6)	C(1)-C(2)	1.496(5)
Zr(1)-Zr(1)#3	3.5344(8)	C(2)-C(7)	1.371(6)
Zr(1)-Zr(1)#1	3.5344(8)	C(2)-C(3)	1.375(5)
Zr(2)-O(2)#4	2.063(3)	C(3)-C(4)	1.388(5)
Zr(2)-O(2)	2.063(3)	C(3)-H(3)	0.9300
Zr(2)-O(4)#5	2.210(2)	C(4)-C(5)	1.381(5)
Zr(2)-O(4)#6	2.210(2)	C(4)-H(4)	0.9300
Zr(2)-O(4)#4	2.210(2)	C(5)-C(6)	1.385(5)
Zr(2)-O(4)	2.210(2)	C(5)-C(8)	1.500(5)
Zr(2)-O(1)	2.338(3)	C(6)-C(7)	1.383(5)
Zr(2)-O(1)#4	2.338(3)	C(6)-H(6)	0.9300
Zr(2)-Zr(1)#1	3.5136(7)	O(2)-Zr(1)-O(2)#1	91.44(17)

Zr(2)-Zr(1)#4	3.5136(7)	O(2)-Zr(1)-O(5)	144.80(10)
Zr(2)-Zr(1)#3	3.5136(7)	O(2)#1-Zr(1)-O(5)	96.86(13)
O(2)-Zr(1)-O(5)#2	96.86(13)	O(5)-Zr(1)-Zr(1)#3	175.81(8)
O(2)#1-Zr(1)-O(5)#2	144.80(10)	O(5)#2-Zr(1)-Zr(1)#3	87.20(10)
O(5)-Zr(1)-O(5)#2	95.8(2)	O(1)-Zr(1)-Zr(1)#3	97.29(8)
O(2)-Zr(1)-O(1)	72.52(11)	O(1)#3-Zr(1)-Zr(1)#3	37.92(6)
O(2)#1-Zr(1)-O(1)	69.31(9)	O(3)-Zr(1)-Zr(1)#3	103.85(8)
O(5)-Zr(1)-O(1)	78.60(12)	O(3)#2-Zr(1)-Zr(1)#3	111.71(7)
O(5)#2-Zr(1)-O(1)	145.66(9)	Zr(2)-Zr(1)-Zr(1)#3	59.805(6)
O(2)-Zr(1)-O(1)#3	69.31(9)	Zr(2)#1-Zr(1)-Zr(1)#3	59.805(6)
O(2)#1-Zr(1)-O(1)#3	72.52(11)	O(2)-Zr(1)-Zr(1)#1	82.30(8)
O(5)-Zr(1)-O(1)#3	145.66(9)	O(2)#1-Zr(1)-Zr(1)#1	31.41(7)
O(5)#2-Zr(1)-O(1)#3	78.60(12)	O(5)-Zr(1)-Zr(1)#1	87.20(10)
O(1)-Zr(1)-O(1)#3	124.17(15)	O(5)#2-Zr(1)-Zr(1)#1	175.81(8)
O(2)-Zr(1)-O(3)	78.57(10)	O(1)-Zr(1)-Zr(1)#1	37.92(6)
O(2)#1-Zr(1)-O(3)	143.13(9)	O(1)#3-Zr(1)-Zr(1)#1	97.29(8)
O(5)-Zr(1)-O(3)	74.36(11)	O(3)-Zr(1)-Zr(1)#1	111.71(7)
O(5)#2-Zr(1)-O(3)	72.04(10)	O(3)#2-Zr(1)-Zr(1)#1	103.85(8)
O(1)-Zr(1)-O(3)	73.84(9)	Zr(2)-Zr(1)-Zr(1)#1	59.805(6)
O(1)#3-Zr(1)-O(3)	132.98(11)	Zr(2)#1-Zr(1)-Zr(1)#1	59.805(6)
O(2)-Zr(1)-O(3)#2	143.13(9)	Zr(1)#3-Zr(1)-Zr(1)#1	90.0
O(2)#1-Zr(1)-O(3)#2	78.57(10)	O(2)#4-Zr(2)-O(2)	92.48(17)
O(5)-Zr(1)-O(3)#2	72.03(10)	O(2)#4-Zr(2)-O(4)#5	143.53(7)
O(5)#2-Zr(1)-O(3)#2	74.36(11)	O(2)-Zr(2)-O(4)#5	84.84(9)
O(1)-Zr(1)-O(3)#2	132.98(11)	O(2)#4-Zr(2)-O(4)#6	84.84(9)
O(1)#3-Zr(1)-O(3)#2	73.84(9)	O(2)-Zr(2)-O(4)#6	143.53(7)
O(3)-Zr(1)-O(3)#2	128.95(13)	O(4)#5-Zr(2)-O(4)#6	117.84(12)
O(2)-Zr(1)-Zr(2)	31.72(7)	O(2)#4-Zr(2)-O(4)#4	84.84(9)
O(2)#1-Zr(1)-Zr(2)	81.80(8)	O(2)-Zr(2)-O(4)#4	143.53(7)
O(5)-Zr(1)-Zr(2)	116.03(8)	O(4)#5-Zr(2)-O(4)#4	76.50(13)
O(5)#2-Zr(1)-Zr(2)	121.02(9)	O(4)#6-Zr(2)-O(4)#4	72.57(14)
O(1)-Zr(1)-Zr(2)	40.92(8)	O(2)#4-Zr(2)-O(4)	143.53(7)
O(1)#3-Zr(1)-Zr(2)	95.15(6)	O(2)-Zr(2)-O(4)	84.84(9)
O(3)-Zr(1)-Zr(2)	71.07(7)	O(4)#5-Zr(2)-O(4)	72.57(14)
O(3)#2-Zr(1)-Zr(2)	159.63(7)	O(4)#6-Zr(2)-O(4)	76.50(13)
O(2)-Zr(1)-Zr(2)#1	81.80(8)	O(4)#4-Zr(2)-O(4)	117.84(12)
O(2)#1-Zr(1)-Zr(2)#1	31.72(7)	O(2)#4-Zr(2)-O(1)	70.60(6)
O(5)-Zr(1)-Zr(2)#1	121.02(9)	O(2)-Zr(2)-O(1)	70.60(6)
O(5)#2-Zr(1)-Zr(2)#1	116.03(8)	O(4)#5-Zr(2)-O(1)	140.09(7)
O(1)-Zr(1)-Zr(2)#1	95.15(6)	O(4)#6-Zr(2)-O(1)	74.26(9)
O(1)#3-Zr(1)-Zr(2)#1	40.92(8)	O(4)#4-Zr(2)-O(1)	140.09(7)
O(3)-Zr(1)-Zr(2)#1	159.63(7)	O(4)-Zr(2)-O(1)	74.26(9)
O(3)#2-Zr(1)-Zr(2)#1	71.07(7)	O(2)#4-Zr(2)-O(1)#4	70.60(6)
Zr(2)-Zr(1)-Zr(2)#1	89.32(2)	O(2)-Zr(2)-O(1)#4	70.60(6)

O(2)-Zr(1)-Zr(1)#3	31.41(7)	O(4)#5-Zr(2)-O(1)#4	74.26(9)
O(2)#1-Zr(1)-Zr(1)#3	82.30(8)	O(4)#6-Zr(2)-O(1)#4	140.09(7)
O(4)#4-Zr(2)-O(1)#4	74.26(9)	Zr(1)-Zr(2)-Zr(1)#3	60.391(12)
O(4)-Zr(2)-O(1)#4	140.09(7)	Zr(1)#4-Zr(2)-Zr(1)#3	60.391(12)
O(1)-Zr(2)-O(1)#4	122.61(14)	Zr(1)-O(1)-Zr(1)#1	104.16(12)
O(2)#4-Zr(2)-Zr(1)#1	31.85(3)	Zr(1)-O(1)-Zr(2)	100.22(10)
O(2)-Zr(2)-Zr(1)#1	82.94(7)	Zr(1)#1-O(1)-Zr(2)	100.2
O(4)#5-Zr(2)-Zr(1)#1	166.38(6)	Zr(1)-O(1)-H(1)	113.5(15)
O(4)#6-Zr(2)-Zr(1)#1	75.75(6)	Zr(1)#1-O(1)-H(1)	113.5(15)
O(4)#4-Zr(2)-Zr(1)#1	110.44(6)	Zr(2)-O(1)-H(1)	123(3)
O(4)-Zr(2)-Zr(1)#1	112.12(7)	Zr(2)-O(2)-Zr(1)	116.43(8)
O(1)-Zr(2)-Zr(1)#1	38.86(4)	Zr(2)-O(2)-Zr(1)#3	116.43(8)
O(1)#4-Zr(2)-Zr(1)#1	95.95(6)	Zr(1)-O(2)-Zr(1)#3	117.17(13)
O(2)#4-Zr(2)-Zr(1)	82.94(7)	C(8)-O(3)-Zr(1)	136.2(2)
O(2)-Zr(2)-Zr(1)	31.85(3)	C(8)-O(4)-Zr(2)	130.0(2)
O(4)#5-Zr(2)-Zr(1)	110.44(6)	C(1)#7-N(1)-C(1)	119.9(4)
O(4)#6-Zr(2)-Zr(1)	112.12(7)	N(1)-C(1)-C(1)#8	120.0(2)
O(4)#4-Zr(2)-Zr(1)	166.38(6)	N(1)-C(1)-C(2)	113.3(3)
O(4)-Zr(2)-Zr(1)	75.75(6)	C(1)#8-C(1)-C(2)	126.65(18)
O(1)-Zr(2)-Zr(1)	38.86(4)	C(7)-C(2)-C(3)	119.4(3)
O(1)#4-Zr(2)-Zr(1)	95.95(6)	C(7)-C(2)-C(1)	122.5(3)
Zr(1)#1-Zr(2)-Zr(1)	60.391(12)	C(3)-C(2)-C(1)	117.6(3)
O(2)#4-Zr(2)-Zr(1)#4	31.85(3)	C(2)-C(3)-C(4)	120.2(4)
O(2)-Zr(2)-Zr(1)#4	82.94(7)	C(2)-C(3)-H(3)	119.9
O(4)#5-Zr(2)-Zr(1)#4	112.12(7)	C(4)-C(3)-H(3)	119.9
O(4)#6-Zr(2)-Zr(1)#4	110.44(6)	C(5)-C(4)-C(3)	120.5(4)
O(4)#4-Zr(2)-Zr(1)#4	75.75(6)	C(5)-C(4)-H(4)	119.7
O(4)-Zr(2)-Zr(1)#4	166.38(6)	C(3)-C(4)-H(4)	119.7
O(1)-Zr(2)-Zr(1)#4	95.95(6)	C(4)-C(5)-C(6)	118.9(3)
O(1)#4-Zr(2)-Zr(1)#4	38.86(4)	C(4)-C(5)-C(8)	119.4(3)
Zr(1)#1-Zr(2)-Zr(1)#4	60.391(12)	C(6)-C(5)-C(8)	121.6(3)
Zr(1)-Zr(2)-Zr(1)#4	90.68(2)	C(7)-C(6)-C(5)	120.1(4)
O(2)#4-Zr(2)-Zr(1)#3	82.94(7)	C(7)-C(6)-H(6)	119.9
O(2)-Zr(2)-Zr(1)#3	31.85(3)	C(5)-C(6)-H(6)	119.9
O(4)#5-Zr(2)-Zr(1)#3	75.75(6)	C(2)-C(7)-C(6)	120.8(4)
O(4)#6-Zr(2)-Zr(1)#3	166.38(6)	C(2)-C(7)-H(7)	119.6
O(4)#4-Zr(2)-Zr(1)#3	112.12(7)	C(6)-C(7)-H(7)	119.6
O(4)-Zr(2)-Zr(1)#3	110.44(6)	O(4)-C(8)-O(3)	125.9(3)
O(1)-Zr(2)-Zr(1)#3	95.95(6)	O(4)-C(8)-C(5)	118.6(3)
O(1)#4-Zr(2)-Zr(1)#3	38.86(4)	O(3)-C(8)-C(5)	115.5(3)
Zr(1)#1-Zr(2)-Zr(1)#3	90.68(2)		

Symmetry transformations used to generate equivalent atoms:

#1 y+1/4, -x+3/4,-z+1/4 #2 -y+3/4,-x+3/4,-z+1/4 #3 -y+3/4,x-1/4,-z+1/4 #4 -x+1,-y+1/2,z+0 #5 x,-y+1/2,z #6 -x+1,y,z #7 -x,y,z #8 x,-y+1,-z

Table S3. Gas adsorption data for **JLU-MOF60**.

Gas	Ads. Amount (cm^3 g^{-1})/273 K	Ads. Amount (cm^3 g^{-1})/298 K
C_2H_2	149	99
C_2H_4	124	80
C_2H_6	146	112
C_3H_8	145	133

Table S4 Comparison of $Cr_2O_7^{2-}$ detection ability of **JLU-MOF60** with MOFs.

MOFs materials	time	$K_{SV}(M^{-1})$	Recyclability	Solvent	Ref.
$[(CH_3)_2NH_2]_6[Cd_3L(H_2O)_2]\cdot 12H_2O$		9.19×10^5		water	1
NUM-5		9.4×10^4	Yes	water	2
$[Cd(TIPA)_2(ClO_4^-)_2]\cdot(DMF)_3(H_2O)$		7.15×10^4		water	3
JLU-MOF60	**seconds**	**5.91×10^4**	**Yes**	**water**	**This work**
$[Eu_2Na(Hpddb)(pddb)_2(CH_3COO)_2]\cdot 2.5(DMA)$	seconds	6.45×10^3	Yes	DMF	4
$\{[Cd_3(HL)_2(H_2O)_3]\cdot 3H_2O\cdot 2CH_3CN\}n$		6.99×10^3	Yes	water	5
$[Zn_2(TPOM)(NDC)_2]\cdot 3.5H_2O$		9.21×10^3		water	6
NU-1000	seconds	1.34×10^4	Yes	water	7
JLU-MOF50	seconds	4.99×10^4	Yes	water	8
BUT-39	seconds	1.57×10^4	Yes	water	9
$[Zn_7(TPPE)_2(SO_4^{2-})_7](DMF\cdot H_2O)$	seconds	1.09×10^4		water	10
$[Eu_2(H_2O)(DCPA)_3]_n$		8.7×10^3	Yes	water	11
$[Eu(Himdc)(ina)(H_2O)]_n$		2.46×10^3		water	12
$[Eu_2(tpbpc)_4\cdot CO_3\cdot 4H_2O]\cdot DMF$		1.04×10^4	Yes	water	13
$[Eu(L)(HCOO)(H_2O)]_n$		2.76×10^4	Yes	water	14
$[Tb(L)(HCOO)(H_2O)]_n$		2.13×10^4	Yes	water	14
Eu-MOF		1.55×10^4		water	15
$\{[Zn(L)(bpe)]\cdot DMF\}_n$		7.91×10^3	Yes	DMF	16
Zn-MOF-1	seconds	2.07×10^4	Yes	water	17
$[Zn_2(TPOM)(NH_2\text{-}BDC)_2]\cdot 4H_2O$	seconds	7.59×10^3	Yes	DMF	18
$[Zn_2(TPOM)(BDC)_2]\cdot 4H_2O$	seconds	4.45×10^3	Yes	DMF	18
$[Cd(L)(TPOM)_{0.75}].x\ S$	seconds	1.35×10^4	Yes	water	19
534-MOF-Tb	seconds	1.37×10^4	Yes	water	20
BUT-28	seconds	1.02×10^5	Yes	water	21

Table S5 Comparison of $Cr_2O_7^{2-}$ adsorption ability of **JLU-MOF60** with other MOFs.

MOF based Adsorbents	Maximum Capacity(mg g^{-1})	Ref.
ZJU-101	245	22
BUT-39	215	9
ABT·2ClO_4	214	23
[Ag(L^{243})](CF_3CO_2)(H_2O)	207	24
MOR-2	193	25
MOR-2-HA	162	25
L-SO_4	166	26
JLU-MOF60	**149**	**This work**
1-Br	128	27
[Cd(TIPA)$_2$(ClO_4^-)$_2$]·(DMF)·3(H_2O)	116	3
BUC-17	121	28
FIR-54	103	29
JLU-MOF50	92	8
NU-1000	76	7
FIR-53	74	29
SLUG-35	68	30
1-ClO_4	63	31
SLUG-21	60	32
PCN-134	57	33
MOF-867	53	34
{Cu_2[CuCl(TTCA)(H_2O)$_2$]}·NO_3·4DMA·6H_2O	68	35

Table S6 Comparison of $Cr_2O_7^{2-}$ photocatalytic reduction ability of **JLU-MOF60** with reported photocatalysts.

Catalysts	C_0 (ppm)	$C_{cat.}$ (mg)	pH	Time (min)	Reductive rate (%)	κ (min^{-1})	Ref.
CuS/MIL-125(Ti)	48	25		70		0.0101	36
MoS_2/MIL125(Ti)	48	25		70		0.0060	36
CdS/MIL-125(Ti)	48	25		70		0.0058	36
Ag_2S/MIL-125(Ti)	48	25		70		0.0035	36
UiO-66(NH_2)	10	20	2	80	97		37
PCN-134-22%	100	10	6	75	88.5		33
TiO_2	100	10	6	75	24.1		33
MOF-525	100	10	6	75	61.9		33
NH_2-MIL-125(Ti)	48	20	2	60	97		38
NNU-36	40	15	2	60	95.3	0.0471	39
NH_2-MIL-88B (Fe)	8	20	2	40	100		40
Pd@UiO-66(NH_2)	10	20	2	90	99		41
MIL-68(In)-NH_2	40	20	6	180	97		42
$[Cu_2I_2(BPEA)](DMF)_4$	10	15	3	10	95		43
B100G100	10	50	2	120	96	0.099	44
BUC-21	10	15	2	30	96		45
$[Cd(4\text{-}Hptz)_2\cdot(H_2O)_2Cl_2]_n$	10	7	3	50	100	0.04818	46
$[Cu(btx)_2(ClO_4)_2]_n$	10	7	3	70	92.17	0.02953	46
$[Cu(btx)(ClO_4)]_n$	10	7	3	60	82.92	0.02175	46
TPB-BTCOF	10	10	7	75	99		47
TAPT-BTCOF	10	10	7	105	99		47
TPB-TPCOF	10	10	7	105	80		47
Phlo-POF	6	9	3	60	100		48
JLU-MOF60	**80**	**10**	**6**	**70**	**98**	**0.056**	**This work**

Table S7 Comparison of anions capture ability of **JLU-MOF60** with other cationic MOFs.

MOFs materials	Anions	Max Capture (mg g^{-1})	Ref.
$[Ag(bipy)]NO_3$	ReO_4^-	786	49
SCU-101	ReO_4^-	217	50
JLU-MOF60	**$Cr_2O_7^{2-}$**	**149**	**This work**
SCU-8	ReO_4^-	45	51
1-ClO4	CrO_4^{2-}	63	52
SLUG-21	CrO_4^{2-}	60	53
$\{[Cd(L)_2(H_2O)_2]\cdot(H_2O)_2\cdot(ClO_4)_2\}$	MO	60	54

References

1. B.-B. Lu, W. Jiang, J. Yang, Y.-Y. Liu and J.-F. Ma, ACS *Appl. Mater. Interfaces,* 2017, **9**, 39441-39449.
2. Z.-Q. Yao, G.-Y. Li, J. Xu, T.-L. Hu and X.-H. Bu, *Chem. Eur. J.*, 2018, **24**, 3192-3198.
3. H.-R. Fu, Y. Zhao, Z. Zhou, X.-G. Yang and L.-F. Ma, *Dalton Trans.*, 2018, **47**, 3725-3732.
4. S. Xu, J.-J. Shi, B. Ding, Z.-Y. Liu, X.-G. Wang, X.-J. Zhao and E.-C. Yang, *Dalton Trans.*, 2019, **48**, 1823-1834.
5. W.-Q. Tong, W.-N. Liu, J.-G. Cheng, P.-F. Zhang, G.-P. Li, L. Hou and Y.-Y. Wang, *Dalton Trans.*, 2018, **47**, 9466-9473.
6. R. Lv, H. Li, J. Su, X. Fu, B.-Y. Yang, W. Gu and X. Liu, *Inorg. Chem.*, 2017, **56**, 12348-12356.
7. Z.-J. Lin, H.-Q. Zheng, H.-Y. Zheng, L.-P. Lin, Q. Xin and R. Cao, *Inorg. Chem.*, 2017, **56**, 14178-14188.
8. X. D. Sun, S. Yao, C. Yu, G. H. Li, C. S. Liu, Q. S. Huo and Y. L. Liu, *J. Mater. Chem. A*, 2018, **6**, 6363-6369.
9. T. He, Y.-Z. Zhang, X.-J. Kong, J. M. Yu, X.-L. Lv, Y. F. Wu, Z.-J. Guo and J.-R. Li, *ACS Appl. Mater. Interfaces*, 2018, **10**, 16650-16659.
10. X.-X. Wu, H.-R. Fu, M.-L. Han, Z. Zhou and L. F. Ma, *Cryst. Growth Des.*, 2017, **17**, 6041-6048.
11. H. M. He, S.- H. Chen, D.-Y. Zhang, R. Hao, C. Zhang, E.-C. Yang and X.-J. Zhao, *Dalton Trans.*, 2017, **46**, 13502-13509.
12. L.-H. Liu, X.-T. Qiu, Y.-J. Wang, Q. Shi, Y.-Q. Sun and Y.-P. Chen, *Dalton Trans.*, 2017, **46**, 12106-12113.
13. J. J. Liu, G. F. Ji, J. N. Xiao and Z. L. Liu, *Inorg. Chem.*, 2017, **56**, 4197- 4205.
14. Z. Sun, M. Yang, Y. Ma and L. C. Li, *Cryst. Growth Des.*, 2017, **17**, 4326-4335.
15. Y.-L. Gai, Q. Guo, X.-Y, Zhao, Y. Chen, S. Liu, Y. Zhang, C.-X. Zhuo, C. Yao and K.-C. Xiong, *Dalton Trans.*, 2018, **47**, 12051-12055.
16. Z. W. Chen, X. N. Mi, S. N. Wang, J. Lu, Y. W. Li, D. C. Li, J. M. Dou, *J. Solid State Chem.*, 2018, **261**, 75-85.
17. X.-Y. Guo, F. Zhao, J.-J. Liu, Z.-L. Liu and Y.-Q. Wang, *J. Mater. Chem. A*, 2017, **5**, 20035-20043.
18. R. Lv, J. Wang, Y. Zhang, H. Li, L. Yang, S. Liao, W. Gu and X. Liu, *J. Mater. Chem. A*, 2016, **4**, 15494-15500.
19. Y. Zhao, X. Xu, L. Qiu, X. Kang, L. Wen and B. Zhang, *ACS Appl. Mater. Interfaces*, 2017, **9**, 15164-15175.
20. M. Chen, W.-M. Xu, J.-Y. Tian, H. Cui, J.-X. Zhang, C.-S. Liu and M. Du, *J. Mater. Chem. C*, 2017, **5**, 2015-2021.
21. M.-M. Xu, X.-J. Kong, T. He, X.-Q. Wu, L.-H. Xie and J.-R. Li, *Inorg. Chem.*, 2018, **57**, 14260-14268.
22. Q. Zhang, J. Yu, J. Cai, L. Zhang, Y. Cui, Y. Yang, B. Chen and G. Qian, *Chem. Commun.*, 2015, **51**, 14732-14734.
23. X. Li, H. Xu, F. Kong and R. Wang, *Angew. Chem., Int. Ed.*, 2013, **52**, 13769-13773.
24. C.-P. Li, H. Zhou, S. Wang, J. Chen, Z.-L. Wang and M. Du, *Chem. Commun.*, 2017, **53**, 9206-9209.
25. S. Rapti, D. Sarma, S. A. Diamantis, E. Skliri, G. S. Armatas, A. C. Tsipis, Y. S. Hassan, M.

Alkordi, C. D. Malliakas, M. G. Kanatzidis, T. Lazarides, J. C. Plakatouras and M. J. Manos, *J. Mater. Chem. A*, 2017, **5**, 14707-14719.

26. A. V. Desai, B. Manna, A. Karmakar, A. Sahu and S. K. Ghosh, *Angew. Chem. Int. Ed.*, 2016, **55**, 7811-7815.
27. X.-X. Lv, L.-L. Shi, K. Li, B.-L. Li and H.-Y. Li, *Chem. Commun.*, 2017, **53**, 1860-1863.
28. J. Guo, J. J. Li and C. C. Wang, *J. Environ. Chem. Eng.*, 2019, **7**, 102909.
29. H.-R. Fu, Z.-X. Xu, and J. Zhang, *Chem. Mater.*, 2015, **27**, 205-210.
30. H. Fei, C. S. Han, J. C. Robins and S. R. J. Oliver, *Chem. Mater.*, 2013, **25**, 647-652.
31. P. F. Shi, B. Zhao, G. Xiong, Y. L. Hou and P. Cheng, *Chem. Commun.*, 2012, **48**, 8231-8233.
32. H. Fei, M. R. Bresler and S. R. J. Oliver, *J. Am. Chem. Soc.*, 2011, **133**, 11110-11113.
33. S. Yuan, J.-S. Qin, L. Zou, Y.-P. Chen, X. Wang, Q. Zhang and H.-C. Zhou, *J. Am. Chem. Soc.*, 2016, **138**, 6636-6642.
34. K. M. Choi, H. M. Jeong, J. H. Park, Y.-B. Zhang, J. K. Kang and O. M. Yaghi, *ACS Nano*, 2014, **8**, 7451-7457.
35. L. Ma, J. Yang, B.-B. Lu, C.-P. Li and J.-F. Ma, *Inorg. Chem.*, 2018, **57**, 11746-11752.
36. H. Wang, X. Z. Yuan, Y. Wu, X. H. Chen, L. J. Leng and G. M. Zeng, *RSC Adv.*, 2015, **5**, 32531-32535.
37. L. J. Shen, S. J. Liang, W. M. Wu, R. W. Liang and L. Wu, *Dalton Trans.*, 2013, **42**, 13649-13657.
38. H. Wang, X. Z. Yuan, Y. Wu, G. M. Zeng, X. H. Chen, L. J. Leng, Z. B. Wu, L. B. Jiang and H. Li, *J. Hazard. Mater.*, 2015, **286**, 187-194.
39. H. M. Zhao, Q. S. Xia, H. Z. Xing, D. S. Chen and H. Wang, *ACS Sustainable Chem. Eng.*, 2017, **5**, 4449-4456.
40. L. Shi, T. Wang, H. B. Zhang, K. Chang, X. G. Meng, H. M. Liu and J. H. Ye, *Adv. Sci.*, 2015, **2**, 1500006.
41. L. J. Shen, W. M. Wu, R. W. Liang, R. Lin and L. Wu, *Nanoscale*, 2013, **5**, 9374-9382.
42. R. W. Liang, L. J. Shen, F. F. Jing, W. M. Wu, N. Qin, R. Lin and L. Wu, *Appl. Catal. B.,* 2015, **162**, 245-251.
43. D.-M. Chen, C.-X. Sun, C. S. Liu and M. Du, *Inorg. Chem.*, 2018, **57**, 7975-7981.
44. X.-H. Yi, F.-X. Wang, X.-D. Du, P. Wang and C.-C. Wang, *Appl Organometal Chem.*, 2019, **33**, e4621.
45. F. X. Wang, X. H. Yi, C. C. Wang and J. G. Deng, *Chin. J. Catal.*, 2017, **38**, 2141-2149.
46. L. W. Wang, T. Y. Zeng, G. Y. Liao, Q. G. Cheng and Zhiquan Pan, *Polyhedron*, 2019, **157**, 152-162.
47. W. B. Chen, Z. F. Yang, Z. Xie, Y. S. Li, X. Yu, F. L. Lu and Long Chen, *J. Mater. Chem. A*, 2019, **7**, 998-1004.
48. V. Kostas, M. Baikousi, K. Dimos, K. C. Vasilopoulos, I. Koutselas and M. A. Karakassides, *J. Phys. Chem. C*, 2017, **121**, 7303-7311.
49. L. Zhu, C. Xiao, X. Dai, J. Li, D. Gui, D. Sheng, L. Chen, R. Zhou, Z. Chai, T. E. Albrecht-Schmitt and S. Wang, *Environ. Sci. Technol. Lett.*, 2017, **4**, 316-322.
50. L. Zhu, D. P. Sheng, C. Xu, X. Dai, M. A. Silver, J. Li, P. Li, Y. X. Wang, Y. L. Wang, L. H. Chen, C. L. Xiao, J. Chen, R. H. Zhou, C. Zhang, O. K. Farha, Z. F. Chai, T. E. Albrecht-Schmitt and S. A. Wang, *J. Am. Chem. Soc.*, 2017, **139**, 14873-14876.
51. Y. X. Li, Z. X. Yang, Y. H. Wang, Z. L. Bai, T. Zheng, X. Dai, S. T. Liu, D. X. Gui, W. Liu, M.

Chen, L. H. Chen, J. Diwu, L. Y. Zhu, R. H. Zhou, Z. F. Chai, T. E. Albrecht-Schmitt and S. A. Wang, *Nat. Commun.*, 2017, **8**, 1354-1365.

52. P.-F. Shi, B. Zhao, G. Xiong, Y.-L. Hou and P. Cheng, *Chem. Commun.*, 2012, **48**, 8231-8233.
53. H. Fei, M. R. Bresler and S. R. J. Oliver, *J. Am. Chem. Soc.*, 2011, **133**, 11110-11113.
54. K. Maity and K. Biradha, *Cryst. Growth Des.*, 2016, **16**, 3002-3013.